

Research article

Ankit Arora, Pramoda K. Nayak, Tejendra Dixit, Kolla Lakshmi Ganapathi, Ananth Krishnan and Mamidanna Sri Ramachandra Rao*

Stacking angle dependent multiple excitonic resonances in bilayer tungsten diselenide

<https://doi.org/10.1515/nanoph-2020-0034>

Received January 15, 2020; accepted May 3, 2020; published online June 18, 2020

Abstract: We report on multiple excitonic resonances in bilayer tungsten diselenide (BL-WSe₂) stacked at different angles and demonstrate the use of the stacking angle to control the occurrence of these excitations. BL-WSe₂ with different stacking angles were fabricated by stacking chemical vapour deposited monolayers and analysed using photoluminescence measurements in the temperature range 300–100 K. At reduced temperatures, several excitonic features were observed and the occurrences of these excitonic resonances were found to be stacking angle dependent. Our results indicate that by controlling the stacking angle, it is possible to excite or quench higher order excitations to tune the excitonic flux in optoelectronic devices. We attribute the presence/absence of

multiple higher order excitons to the strength of interlayer coupling and doping effect from SiO₂/Si substrate. Understanding interlayer excitations will help in engineering excitonic devices and give an insight into the physics of many-body dynamics.

Keywords: 2D transition metal dichalcogenides; bilayer WSe₂; excitonic device; many-body dynamics; multiple excitonic resonances; stacking angle.

PACS: 78.67.-n; 71.35.-y.

1 Introduction

Transition metal dichalcogenides (TMDs) with the chemical formula MX₂ (M = transition metal and X = chalcogen) are a class of two-dimensional (2D) materials beyond graphene, which have attracted much attention recently because of their interesting optical properties [1, 2]. Monolayer (1L) TMDs are direct bandgap semiconductors with excellent quantum confinement, broken inversion symmetry and reduced dielectric screening resulting in the formation of strong coulomb bound electron-hole pair, called excitons [3, 4]. Hence, light-matter interactions in these systems are primarily governed by the excitonic effects, which have been exploited to develop exciton-based devices [5–9]. Apart from this two body complex, 1L-TMDs also exhibit higher-order excitations namely, three body complex called charged exciton or trion [10], four body complex called biexciton [11], and so on [12, 13]. These higher order excitations show distinct excitation power dependence [14–16], lifetime [11], spatial distribution [17, 18], and have specific spin-valley configurations [19–21] which make them useful for novel quantum optoelectronic applications. However, external control of these excitations in 1L-TMDs have remained a major challenge and restricted their practical applicabilities.

Bilayer (BL) systems comprising of two monolayers of same or different TMDs have drawn lots of interest towards designing novel quantum materials due to fascinating emergent properties [22–27]. The key control knob

*Corresponding author: Mamidanna Sri Ramachandra Rao, Department of Physics and Materials Science Research Centre, Indian Institute of Technology Madras, Chennai, 600036, India, and Nano Functional Materials Technology Centre, Indian Institute of Technology Madras, Chennai, 600036, India, E-mail: msrrao@iitm.ac.in. <https://orcid.org/0000-0002-7806-2151>

Ankit Arora: Centre for NEMS and Nano Photonics, Department of Electrical Engineering, Indian Institute of Technology Madras, Chennai, 600036, India; Department of Physics and Materials Science Research Centre, Indian Institute of Technology Madras, Chennai, 600036, India; and Nano Functional Materials Technology Centre, Indian Institute of Technology Madras, Chennai, 600036, India. <https://orcid.org/0000-0003-4899-1336>

Pramoda K. Nayak and Kolla Lakshmi Ganapathi: Department of Physics and Materials Science Research Centre, Indian Institute of Technology Madras, Chennai, 600036, India, E-mail: pnayak@iitm.ac.in (P.K. Nayak)

Tejendra Dixit: Department of Physics and Materials Science Research Centre, Indian Institute of Technology Madras, Chennai, 600036, India; Department of Electronics and Communication Engineering, Indian Institute of Information Technology D&M, Kancheepuram, Chennai, 600127, India

Ananth Krishnan: Centre for NEMS and Nano Photonics, Department of Electrical Engineering, Indian Institute of Technology Madras, Chennai, 600036, India, E-mail: ananthk@iitm.ac.in

for designing these materials is the stacking angle dependent interlayer coupling which can be used as an external degree of freedom to tune their optical and electronic properties [28–31]. Recently, electrically controlled excitonic switching has been demonstrated in BL-TMDs due to the formation of interlayer excitonic species [32–34]. Although some initial work has been done to explore many body effects in BL-TMDs [28, 35, 36], most of these demonstrations are limited only to neutral excitons. However, for better flux control and efficient device applications, it is important to understand all the higher order excitations and their stacking angle dependence in BL-TMD systems.

In the present work, we report on multiple excitonic resonances in BL-WSe₂ on SiO₂/Si substrate stacked at different angles, using temperature dependent photoluminescence (PL) measurements. At temperature ~ 100 K, the presence or absence of these resonances showed strong stacking angle dependence. Excitation power dependent PL measurements confirmed the nature of these resonances as higher order excitations, such as trions and biexcitons, along with neutral excitons. The emission intensities and the peak positions of these higher order excitations, relative to that of the neutral exciton, showed a systematic stacking angle dependence. These observations demonstrated the interlayer nature of these excitations and were attributed to stacking angle dependent interlayer distance and doping efficiency from SiO₂/Si substrate. This study provides an ideal platform for understanding interlayer excitations in BL-TMD systems for engineering excitonic devices and gives an insight into the physics of the many-body dynamics.

2 Materials and methods

Monolayer (1L) WSe₂ flakes were grown on sapphire (001) substrate using low pressure chemical vapour deposition (LPCVD) as reported earlier [37]. The as grown 1L-WSe₂ flakes on sapphire substrate were transferred onto SiO₂/Si substrate with 300 nm oxide thickness using polymethyl methacrylate (PMMA) based transfer process [37]. For the second layer transfer, 1L-WSe₂/SiO₂/Si was used as the substrate in place of SiO₂/Si. In order to reduce any inhomogeneity in the overlapping region caused due to the transfer process, samples were annealed at ~ 600 K for 1 h in Argon atmosphere [37]. As the transfer process was random, bilayer (BL) systems with several stacking angles were obtained and are shown in Fig.S1 of the supplementary information. Stacking angle was measured as clockwise orientation of the top layer with respect to bottom layer with an accuracy of $\sim 2^\circ$. Due to three-fold symmetry of WSe₂ flakes, BL-WSe₂ stacked at angles 0° and 60° have minimum steric hindrance and hence maximum interlayer interaction, while those stacked at angles around 30° have maximum steric hindrance and hence minimum interlayer interaction [28, 29]. Therefore, from several fabricated BL systems, one with asymmetrically stacked at angle 36° and two with symmetrically stacked at angles 0° and 60° were selected for further studies, their corresponding scanning electron microscopy (SEM) images and schematics are shown in Figure 1. The atomic force microscopy measurements using Park Systems NX10 were carried out to determine the thickness of WSe₂ flakes as shown in Fig. S2. An edge step height ~ 0.9 nm at the substrate-bottom layer interface and ~ 0.7 nm at the bottom layer-top layer interface corresponds to thickness of the two constituent 1L-WSe₂. These BL-WSe₂ systems were characterized using room temperature (RT) Raman and temperature dependent PL using a HORIBA LabRAM confocal micro-PL system in back scattering geometry. A laser of wavelength 488 nm, spot size ~ 1 μ m and tunable optical power from ~ 0.3 to 300 μ W was used as the excitation source. For RT measurements, 100 \times objectives were used while for low temperature measurements, long working distance 50 \times objectives were used. All the PL and Raman spectroscopy measurements of BL-WSe₂ samples were carried out at three different locations in the overlap region.

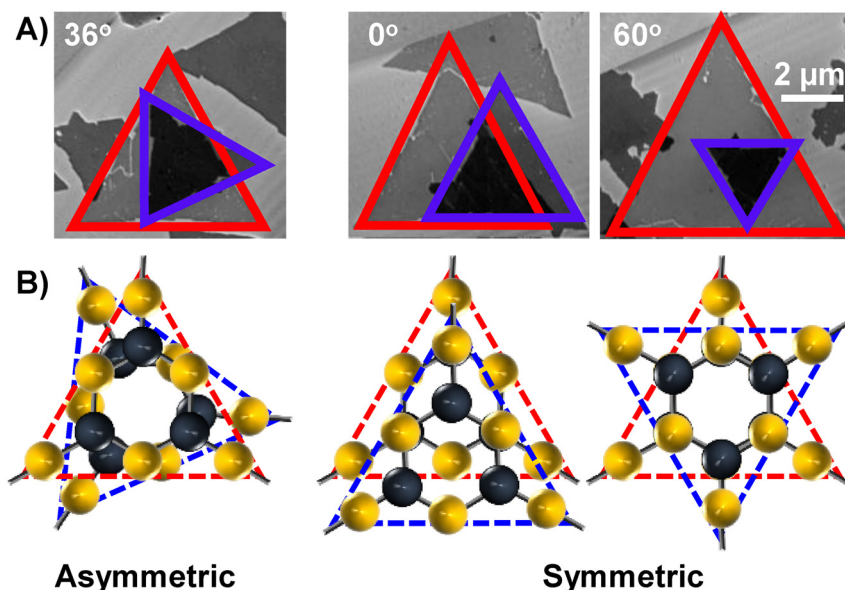


Figure 1: (A) SEM images and (B) Schematic of BL-WSe₂ with asymmetric (36°) and symmetric (0° and 60°) stacking angles. Monolayers marked in red and blue triangles are the bottom and the top layers respectively. Black spheres represent W atoms and yellow spheres represent Se atoms. The schematics have been drawn considering the two centrosymmetric triangles.

3 Results and discussion

As grown 1L-WSe₂ flakes on sapphire and post-transfer on SiO₂/Si were characterized for their optical properties using PL measurements. The RT PL peak of as grown pristine 1L-WSe₂ on sapphire was observed at ~1.59 eV which shifted to ~1.66 eV after transfer to SiO₂/Si substrate due to the stress release and bandgap renormalization after the transfer [38]. Figure 2A shows the RT PL spectra of 1L and the three BL-WSe₂ on SiO₂/Si. The peak PL intensity for all the BL systems was approximately half the intensity of 1L-WSe₂ with negligible change in the peak position. This reduction in the PL intensity was due to the transition from direct bandgap in monolayer to partial indirect bandgap nature in BL systems [28, 39]. Interestingly, these spectra did not show any significant stacking angle dependence. Figure 2B shows the low frequency RT Raman spectra of BL-WSe₂ for different stacking angles. The red curve corresponding to the 60° stacking, shows two modes at ~17.3 and ~29.5 cm⁻¹ which can be attributed respectively to the in-plane shear mode (SM) and out-of-plane layer breathing mode (LBM) [40, 41]. However, in the case of 0° stacking, shown in blue, SM was absent and only LBM was observed, with a slight red shift and peak broadening. The absence of SM was due to its high sensitivity to the atomic alignment and the red shift in LBM was due to reduced restoring force between the layers [41–43]. In the case of 36° stacking, both these modes were quenched due to the lack of strong interlayer interaction. The low frequency Raman spectrum of 1L-WSe₂, shown in black, showed a peak close to 20 cm⁻¹, whose origin is not yet clear and can be attributed to resonant effect arising due to 488 nm excitation wavelength [37]. A similar peak has earlier been reported in MoS₂ at 38 cm⁻¹ for 632 nm excitation [44]. Figure 2C shows the RT Raman spectra of BL-WSe₂ for different stacking angles at higher frequencies. The peak at ~250 cm⁻¹ can be attributed to E_{2g} modes and at ~260 cm⁻¹ to the second order 2LA(M) mode [45]. These modes were found to be relatively

insensitive to the stacking angle. A weak peak at ~308 cm⁻¹ was observed in all the bilayer systems which corresponds to the out-of-plane interlayer coupling mode A₂' and hence was absent in 1L-WSe₂ [45].

Since RT PL spectra were found to be insensitive to stacking angle, temperature dependent PL measurements down to 100 K, were carried out on these BL systems and the corresponding spectra are shown in Fig.S3. It was observed that, with the reduction in temperature, there was a blue shift and a gradual reduction in the PL intensity of 1L as well as all the BL-WSe₂ systems, which can be attributed to the presence of optically dark exciton in WSe₂ [46, 47]. Further, at temperatures below 150 K, the PL line shape of asymmetrically and symmetrically stacked BL-WSe₂ systems were different. Figure 3A shows the PL spectrum of asymmetrically stacked BL-WSe₂ at 100 K obtained using 66 μW excitation power. The PL spectrum clearly showed the emergence of distinct emission features which indicated the presence of multiple excitonic states. Deconvolution of the PL spectrum into the constituent Gaussian curves showed three dominant peaks marked as X₀ (red), X₁ (green), and X₂ (blue). Similar excitonic features were observed in the case of 1L-WSe₂ on SiO₂/Si but were absent in the case of 1L-WSe₂ on sapphire substrate as shown in the inset of Figure 3A. Therefore, it can be inferred that the emergence of these distinct emission features was a substrate dependent effect, in this case, due to the excess carriers from SiO₂/Si substrate coming from the interface impurities or dangling bonds resulting in the doping of WSe₂ flakes [28, 38, 48].

In order to understand the nature of these excitonic states, power dependent PL measurements were performed with the excitation power (P_{Ex}) varying from 0.03 to 240 μW. A broad low energy emission for P_{Ex} ~ 0.03 μW was observed as shown in Fig. S4, which was negligible for higher P_{Ex} and can be attributed to localized excitons [15]. Figure 3B shows the logarithmic plot of the PL intensities (I)

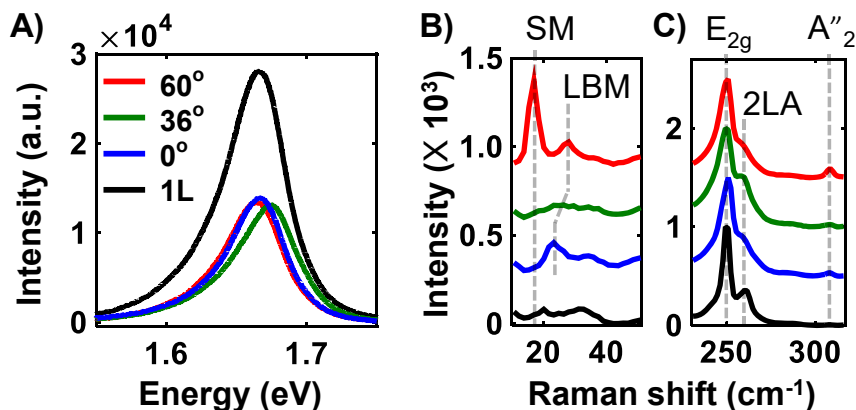


Figure 2: (A) Room temperature PL spectra; (B) Low frequency Raman spectra and (C) High frequency Raman spectra of 1L and BL-WSe₂ for different stacking angles. The characteristic low frequency shear mode (SM) and layer breathing mode (LBM) and higher frequency E_{2g}, 2LA, and A₂' modes are marked with vertical dashed lines.

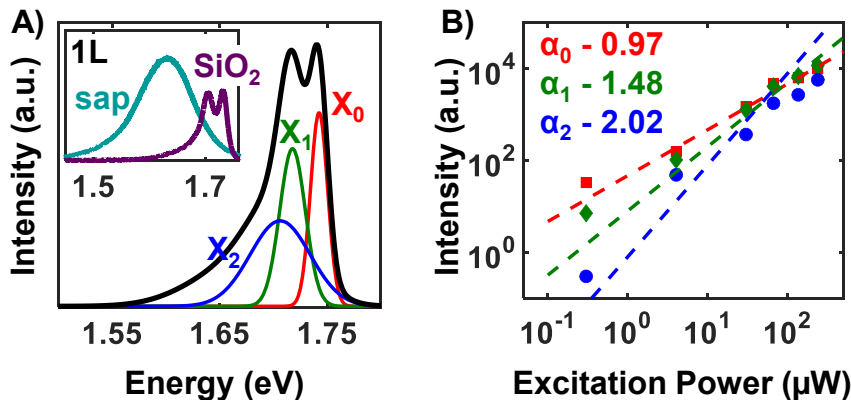


Figure 3: Asymmetrically stacked BL-WSe₂ (36°): (A) PL spectrum (black) at 100 K, obtained using 66 μ W 488 nm excitation. The constituent deconvoluted peaks are marked as X₀ (red) at \sim 1.74 eV, X₁ (green) at \sim 1.72 eV, and X₂ (blue) at \sim 1.70 eV. The inset shows the PL spectra of 1L-WSe₂ on sapphire (sap) and post-transfer on SiO₂/Si substrate at 100 K; and (B) Excitation power dependence of X₀, X₁, and X₂ and their fit to the power law $I \propto P_{Ex}^\alpha$.

for different excitation power (P_{Ex}) of the peaks marked in Figure 3A and their fit to the power law $I \propto P_{Ex}^\alpha$. The slope of the power law fit corresponds to α and has been indicated in the figure. The peak marked as X₀ at \sim 1.74 eV showed almost linear dependence on P_{Ex} with $\alpha \sim 0.97$ and hence can be attributed to neutral exciton [14]. The PL intensities of the other two peaks were observed to increase more steeply with P_{Ex} , thereby indicating their origin to be higher order excitons. The peak marked as X₁ at \sim 1.72 eV showed super-linear behaviour with $\alpha \sim 1.48$ which is a characteristic of the three body complex called trion, consisting of a hole and two electrons [15, 38]. Excess carries from SiO₂/Si resulted in higher electron density in BL-WSe₂ thereby increasing the probability of a neutral exciton to interact with an electron resulting in a negative trion with binding energy \sim 20 meV. The peak at \sim 1.70 eV marked as X₂ showed quadratic behaviour with $\alpha \sim 2.02$ for $P_{Ex} < 100 \mu$ W, however became almost linear for higher P_{Ex} . Based on its quadratic dependence on the excitation power and its position \sim 40 meV below the neutral exciton, the peak X₂ can be attributed to the four body complex called biexciton [36]. The emission intensity saturation at higher P_{Ex} was due to non-radiative decay channel, such as exciton-exciton annihilation at high exciton density [49]. These emission properties of the asymmetrically stacked BL-WSe₂, that is, the peak positions, binding energies, and the power dependence of the neutral exciton, negative trion, and biexciton are similar to that of the 1L-WSe₂. This indicates that, though there is some interlayer interaction between the constituent layers, the asymmetrically stacked BL system is equivalent to two 1L systems. However, the case of symmetrically stacked BL systems were strikingly different from their constituent monolayers and also from that of asymmetrically stacked one.

Figure 4A,C) show the PL spectra of the two symmetrically stacked BL-WSe₂, stacked at 0° and 60° at 100 K,

obtained using 66 μ W excitation power. These PL spectra showed the emergence of several distinct emission features and a red shift of \sim 10 meV with respect to the asymmetrically stacked system. The three peaks labelled as X₀ (red), X₁ (green), and X₂ (blue) correspond to the ones observed in the case of asymmetric stacking, namely, the neutral exciton, negative trion and the biexciton. However, from I versus P_{Ex} plots shown in Figure 4B,D, it was observed that the P_{Ex} dependence of the neutral exciton was reduced to sub-linear from linear and that of the biexciton reduced to 1.28 (1.06) for 60° (0°) from quadratic in the asymmetric case. Moreover, the peaks X₃ to X₅ labelled in Figure 4A,C were not observed in the asymmetrically stacked BL system. The peak marked as X₃, based on its position at 1.65 eV and its super-linear P_{Ex} dependence of \sim 1.24 (1.13) for 0° (60°) as shown in Fig. S5, may be assigned to the exciton-trion complex also known as charged biexciton [12, 13]. This negatively charged five body complex consists of two holes and three electrons with specific spin-valley configuration. Since, the two valence-band holes residing in the same valley is energetically unfavourable, the only possible configuration would consist of a negative-trion bound to an exciton residing in different valleys [13]. Emission peaks at 1.60 eV and below in both the symmetrically stacked systems may be attributed to indirect and localized excitons [39, 15]. Another feeble peak between X₂ and X₃ in the case of 60° was observed, its exact origin is still under investigation. It should be pointed here that the possibility of the formation of moiré superlattice due to the angle measurement tolerance of \sim 2° can be ignored as this effect for TMDs are known to be pronounced for angles $\geq 3.1^\circ$ [50, 51]. Also, the PL measurements at three different locations on the overlapping region were observed to be consistent with an intensity variation within the experimental limits, indicating absence of regions of different stacking created due to moiré superlattice [42]. However, no atomic resolution images were obtained and no local

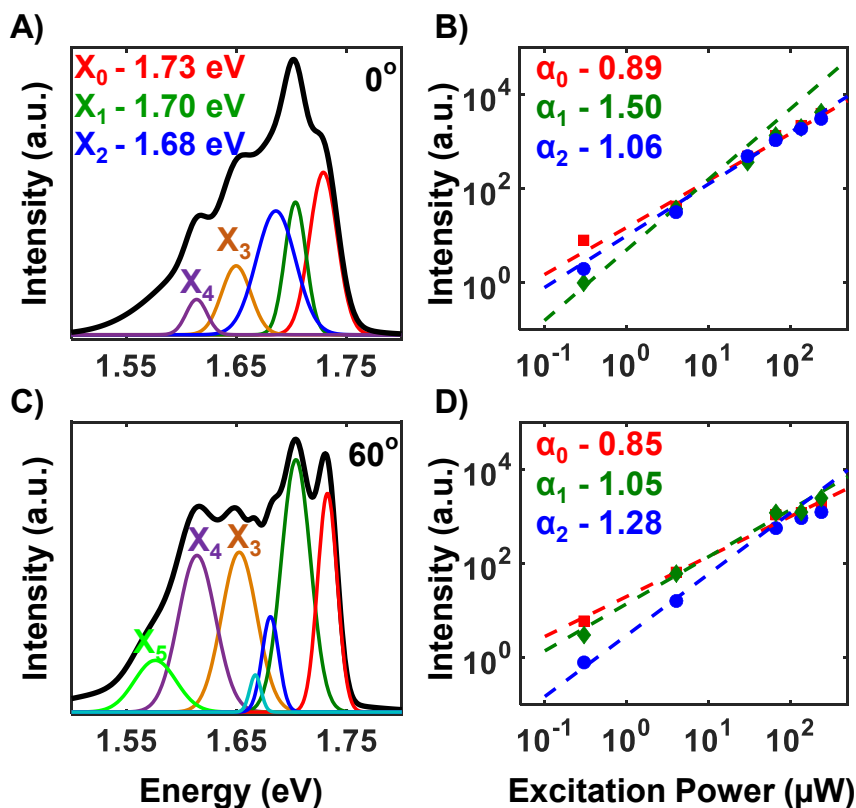


Figure 4: Symmetrically stacked BL-WSe₂: (A & C) PL spectrum (black) at 100 K obtained using 488 nm, 66 μ W excitation for 0° and 60° respectively. The constituent deconvoluted peaks are marked from X_0 to X_5 ; and (B & D) Excitation power dependence of peaks marked as X_0 , X_1 , and X_2 for 0° and 60° respectively, and their fit to the power law $I \propto P_{Ex}^a$.

probe measurements were done on the fabricated bilayer samples as this was beyond the scope of this work.

Therefore, from these observations it is evident that the emission properties and presence/absence of different excitonic states in BL-WSe₂ system is highly sensitive to the stacking angle. Figure 5A shows the intensity ratios and the binding energies of X_1 and X_2 of the three BL systems. The intensity ratio was calculated as the peak emission intensity normalized with their respective neutral exciton intensity. The contribution of both the higher order excitons is more in the case of symmetrically stacked system when

compared to the asymmetrically stacked one. Also, it can be noted that for symmetrically stacked systems, the binding energies of X_1 and X_2 were 30 and 50 meV respectively, which were reduced to 20 and 40 meV in the case of asymmetric stacking. These observed differences may be attributed mainly to two effects: (i) the interlayer coupling and (ii) doping from the substrate. Firstly, due to steric hindrance in the case of asymmetrically stacked BL-WSe₂, the interlayer distance is ~ 0.72 nm, as calculated theoretically in earlier reported work, which reduces to ~ 0.65 nm for symmetrically stacked one [52]. This reduction in interlayer

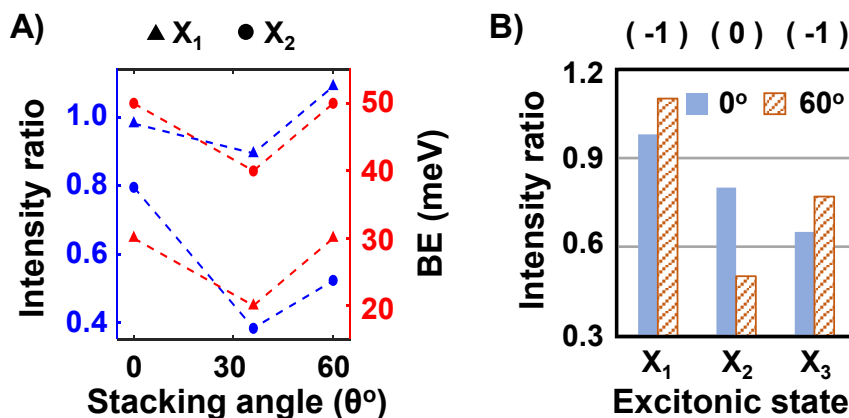


Figure 5: (A) Intensity ratio (the peak emission intensity normalized with respect to the intensity of neutral exciton) and the binding energies (BE) in meV of trion (X_1) marked as \blacktriangle and biexciton (X_2) marked as \bullet of BL-WSe₂ with different stacking angles at 100 K; and (B) Intensity ratio of trion (X_1), biexciton (X_2), and charged-biexciton (X_3) of BL-WSe₂ stacked at 0° and 60° at 100 K. Top axis shows the charge of the species X_1 , X_2 , and X_3 as -1, 0, or neutral and -1 respectively.

distance would result in larger van der Waals force, stronger interlayer coupling and higher exciton density. Secondly, the doping effect from the SiO₂/Si substrate has earlier been shown to depend on the stacking angle [28]. The excess electron transfer from SiO₂/Si is more efficient for stronger interlayer coupling and therefore is maximum in the case of symmetric stacking compared to that in the asymmetric case. These two effects together would give rise to increased carrier density and hence multiple higher order excitonic states in the symmetrically stacked BL systems and quench them in the asymmetrically stacked ones. Further, from a closer analysis of the two symmetrically stacked cases, it can be inferred that the difference in the PL spectrum is mainly due to the difference in relative contributions from the different excitonic states. It was observed that the relative contribution of the charged species, viz., trion and charged biexciton was more in 60° stacking while the neutral biexciton was more in 0° stacking, as shown in Figure 5B. This indicates that the doping effect is more in the case of the 60° compared to that in 0° stacking.

4 Conclusions

In conclusion, multiple excitonic resonances were observed in BL-WSe₂ from temperature dependent PL measurements down to 100 K. The evolution of these excitonic resonances was found to be sensitive to the stacking angle i. e. appear in case of high symmetric stacking, 0° and 60° and disappear in the case of asymmetric stacking, here 36°, an intermediate angle. Excitation power dependent PL measurements at 100 K confirmed the nature of these resonances as higher order excitations such as trions and biexcitons, along with neutral excitons. These higher order excitations showed interlayer nature and their occurrence were attributed to stacking angle dependent interlayer coupling and doping efficiency from SiO₂/Si substrate. This work provides an ideal platform for understanding interlayer excitations in BL-TMD systems for engineering excitonic devices and give an insight into the physics of the many-body dynamics.

Acknowledgment: This work was partially supported by the Department of Science and Technology, Government of India (DST-GoI) that led to the establishment of Nano Functional Materials Technology Centre (NFMTC) (SR/NM/NAT/02-2005 and DST/NM/JIIT-01/2016(C)). P.K.N. acknowledge the financial support from DST-GoI, with sanction order no. SB/S2/RJN-043/2017 under Ram-anujan Fellowship. K.L.G. acknowledge the financial support from DST-GoI, with sanction order no. DST/

INSPIRE/04/2016/001865 under DST INSPIRE Faculty program.

Author contribution: All the authors have accepted responsibility for the entire content of this submitted manuscript and approved submission.

Research funding: This research was funded by the Department of Science and Technology, Government of India (DST-GoI) that led to the establishment of Nano Functional Materials Technology Centre (NFMTC) (SR/NM/NAT/02-2005 and DST/NM/JIIT-01/2016(C)).

Employment or leadership: None declared.

Honorarium: None declared.

Conflict of interest statement: The authors declare no conflicts of interest regarding this article.

References

- [1] K. F. Mak, and J. Shan, *Nat. Photon.*, vol. 10, pp. 216, 2016.
- [2] S. Manzeli, D. Ovchinnikov, D. Pasquier, O. V. Yazyev, and A. Kis, *Nat. Rev. Mater.* vol. 2, pp. 17033, 2017.
- [3] J. Xiao, M. Zhao, Y. Wang, and X. Zhang, *Nanophotonics*, vol. 6, pp. 1309, 2017.
- [4] G. Wang, A. Chernikov, M. M. Glazov, et al., *Rev. Modern Phys.*, vol. 90, 2018, 021001.
- [5] T. Mueller, and E. Malic, *npj 2D Mater. Applic.*, vol. 2, pp. 1, 2018.
- [6] D. Jariwala, V. K. Sangwan, L. J. Lauhon, T. J. Marks, and M. C. Hersam, *ACS Nano*, vol. 8, pp. 1102, 2014.
- [7] J. Pu, and T. Takenobu, *Adv. Mater.*, vol. 30, pp. 1707627, 2018.
- [8] C. Chakraborty, L. Kinnischtzke, K. M. Goodfellow, R. Beams, and A. N. Vamivakas, *Nat. Nanotechnol.*, vol. 10, pp. 507, 2015.
- [9] C. Palacios-Berraquero, M. Barbone, D. M. Kara, et al., *Nat. Commun.*, vol. 7, pp. 12978, 2016.
- [10] K. F. Mak, K. He, C. Lee, et al., *Nat. Mater.*, vol. 12, pp. 207, 2013.
- [11] Y. You, X. X. Zhang, T. C. Berkelbach, M. S. Hybertsen, D. R. Reichman, and T. F. Heinz, *Nat. Phys.*, vol. 11, pp. 477, 2015.
- [12] S. Y. Chen, T. Goldstein, T. Taniguchi, K. Watanabe, and J. Yan, *Nat. Commun.*, vol. 9, pp. 3717, 2018.
- [13] Z. Li, T. Wang, Z. Lu, et al., *Nat. Commun.*, vol. 9, 2018, <https://doi.org/10.1038/s41467-018-05863-5>.
- [14] D. Kaplan, Y. Gong, K. Mills, et al., *2D Mater.*, vol. 3, 2016, Art no. 015005, <https://doi.org/10.1088/2053-1583/3/1/015005>.
- [15] J. Huang, T. B. Hoang, and M. H. Mikkelsen, *Sci. Rep.*, vol. 6, pp. 22414, 2016.
- [16] M. Barbone, A. R.P. Montblanch, D. M. Kara, et al., *Nat. Commun.*, vol. 9, pp. 3721, 2018.
- [17] T. Kato, and T. Kaneko, *ACS Nano*, vol. 10, pp. 9687, 2016.
- [18] Y. Lee, S. J. Yun, Y. Kim, et al., *Nanoscale*, vol. 9, pp. 2272, 2017.
- [19] E. J. Sie, A. J. Frenzel, Y.H. Lee, J. Kong, and N. Gedik, *Phys. Rev. B* vol. 92, pp. 125417, 2015.
- [20] G. Plechinger, P. Nagler, A. Arora, et al., *Nat. Commun.*, vol. 7, pp. 12715, 2016.
- [21] K. Hao, J. F. Specht, P. Nagler, et al., *Nat. Commun.*, vol. 8, pp. 15552, 2017.
- [22] Y. Wang, C. Cong, J. Shang, et al., *Nanoscale Horizons*, vol. 4, pp. 396, 2019.
- [23] S. Das, G. Gupta, and K. Majumdar, *Phys. Rev. B*, vol. 99, pp. 165411, 2019.

- [24] I. C. Gerber, E. Courtade, S. Shree, et al., *Phys. Rev. B*, vol. 99, 2019, Art no. 035443, <https://doi.org/10.1103/PhysRevB.99.035443>.
- [25] C. Jin, E. Y. Ma, O. Karni, E. C. Regan, F. Wang, and T. F. Heinz, *Nat. Nanotechnol.*, vol. 13, pp. 994, 2018.
- [26] Z. Wang, Y. H. Chiu, K. Honz, K. F. Mak, and J. Shan, *Nano Lett.*, vol. 18, pp. 137, 2017.
- [27] A. M. Jones, H. Yu, J. S. Ross, et al., *Nat. Phys.*, vol. 10, pp. 130, 2014.
- [28] S. Huang, X. Ling, L. Liang, et al., *Nano Lett.*, 14, pp. 5500, 2014.
- [29] A. M. van Der Zande, J. Kunstmann, A. Chernikov, et al., *Nano Lett.*, vol. 14, pp. 3869, 2014.
- [30] S. Zheng, L. Sun, X. Zhou, et al., *Adv. Opt. Mater.*, vol. 3, pp. 1600, 2015.
- [31] W. T. Hsu, B. H. Lin, L. S. Lu, et al., *Sci. Adv.*, vol. 5, 2019, <https://doi.org/10.1126/sciadv.aax7407>.
- [32] D. Unuchek, A. Ciarrocchi, A. Avsar, K. Watanabe, T. Taniguchi, and A. Kis, *Nature*, vol. 560, pp. 340, 2018.
- [33] A. Ciarrocchi, D. Unuchek, A. Avsar, K. Watanabe, T. Taniguchi, and A. Kis, *Nat. Photonics*, vol. 13, pp. 131, 2019.
- [34] M. Tahir, P. Krstajić, and P. Vasilopoulos, *Phys. Rev. B*, vol. 98, 2018, Art no. 075429, <https://doi.org/10.1103/PhysRevB.98.075429>.
- [35] T. Deilmann, and K. S. Thygesen, *Nano Lett.*, vol. 18, pp. 1460, 2018.
- [36] Z. He, W. Xu, Y. Zhou, et al., *ACS Nano*, vol. 10, pp. 2176, 2016.
- [37] P. K. Nayak, Y. Horbatenko, S. Ahn, et al., *Acs Nano*, vol. 11, pp. 4041, 2017.
- [38] S. Lippert, L. M. Schneider, D. Renaud, et al., *2D Mater.*, vol. 4, 2017, Art no. 025045, <https://doi.org/10.1088/2053-1583/aa5b21>.
- [39] W. Zhao, R. M. Ribeiro, M. Toh, et al., *Nano Lett.*, vol. 13, pp. 5627, 2013.
- [40] A. A. Poretzky, L. Liang, X. Li, et al., *ACS Nano*, vol. 9, pp. 6333, 2015.
- [41] C. H. Lui, Z. Ye, C. Ji, et al., *Phys. Rev. B*, vol. 91, pp. 165403, 2015.
- [42] S. Huang, L. Liang, X. Ling, et al., *Nano Lett.*, vol. 16, pp. 1435, 2016.
- [43] A. A. Poretzky, L. Liang, X. Li, et al., *ACS Nano*, vol. 10, pp. 2736, 2016.
- [44] J. U. Lee, J. Park, Y. W. Son, and H. Cheong, *Nanoscale*, vol. 7, pp. 3229, 2015.
- [45] W. Zhao, Z. Ghorannevis, K. K. Amara, et al., *Nanoscale*, vol. 5, pp. 9677, 2013.
- [46] X.-X. Zhang, Y. You, S. Y. F. Zhao, and T. F. Heinz, *Phys. Rev. Lett.*, 115, pp. 257403, 2015.
- [47] A. Arora, T. Dixit, K. Anil Kumar, et al., *Appl. Phys. Lett.*, vol. 114, pp. 201101, 2019.
- [48] M. Drüppel, T. Deilmann, P. Krüger, and M. Rohlfing, *Nat. Commun.*, vol. 8, pp. 2117, 2017.
- [49] D. Sun, Y. Rao, G. A. Reider, et al., *Nano Lett.*, vol. 14, pp. 5625, 2014.
- [50] M. H. Naik, and M. Jain, *Phys. Rev. Lett.*, vol. 121, pp. 266401, 2018.
- [51] L. Wang, E. M. Shih, A. Ghiotto, et al., *arXiv preprint arXiv:1910.12147*, 2019.
- [52] J. He, K. Hummer, and C. Franchini, *Phys. Rev. B*, vol. 89, 2014, Art no. 075409, <https://doi.org/10.1103/PhysRevB.89.075409>.

Supplementary material: The online version of this article offers supplementary material <https://doi.org/10.1515/nanoph-2020-0034>.